

SPECIAL PROJECT PROGRESS REPORT

All the following mandatory information needs to be provided. The length should *reflect the complexity and duration* of the project.

Reporting year 2021

Project Title: Near-term Climate Prediction at High Resolution

Computer Project Account: spesiccf

Principal Investigator(s): Etienne Tourigny

Affiliation: Barcelona Supercomputing Center

Name of ECMWF scientist(s) collaborating to the project (if applicable) N/A

Start date of the project: January 2020

Expected end date: December 2021

Computer resources allocated/used for the current year and the previous one (if applicable)

Please answer for all project resources

		Previous year		Current year	
		Allocated	Used	Allocated	Used
High Performance Computing Facility	(units)	66M	66M	66M	2,8M
Data storage capacity	(Gbytes)	60k	52k	60k	82k (cleaning)

Summary of project objectives

The main objective of the first set of experiments (year 1) is to better understand the climate impacts of the observed AMV in order to estimate their predictability. This will be done by performing idealized experiments with EC-Earth3 CGCM in which the North Atlantic SST will be restored towards the observed AMV anomalies. We will particularly focus on the AMV impacts on the occurrence of weather extremes such as Tropical Cyclones, heat waves, and heavy precipitation events. In the second part (year 2), we explore the impact of increasing horizontal resolution on the oceanic and atmospheric domains on seasonal prediction skill of EC-Earth3 through retrospective seasonal predictions of seven months initialized twice every year for the period 1980-2018. Specific emphasis will be made on improvements in simulating Arctic climate variability, and how it affects simulated climate over land areas including Europe, and climate extremes.

Summary of problems encountered

The first long simulations performed with the high-resolution (HR) version of EC-Earth3 used for the second part of this project, revealed an unrealistically cold climate over the North Atlantic sector, strong enough to degrade the skill of the forecasts. To reduce this bias and thus produce better forecasts, a retuning effort of this version of the model has been done during the first implementation period of the project and is described in more detail in the Summary of results section.

In parallel, we have also been improving the in-house reconstruction to be used to initialize the HR seasonal predictions, which assimilates ocean temperatures and salinity from the ocean reanalysis ORAS5. A new protocol was developed to produce these oceanic conditions in such a way to avoid the appearance of a non-stationary bias reported in North Atlantic subsurface temperature of ORAS5 (Tietsche et al., 2020). This new setup is described in the Summary of results section.

Summary of plans for the continuation of the project

The new ocean reconstruction from which the predictions will be initialised is currently in production and expected to be completed in 3 weeks at the time of writing. It assimilates ORAS5 temperature and salinity and follows a new refined strategy developed and tested successfully in the lower resolution of the model to prevent the inclusion of the non-stationary bias in the North Atlantic reported in Tietsche et al. (2020) for ORAS5. As soon as it is finished we will validate the reconstruction against other observational products, and start the production of the seasonal forecasts, which should be completed during this summer. The analysis of the predictions will follow during the final months of the year.

List of publications/reports from the project with complete references

Ruggieri, P., Bellucci, A., Nicolí, D., Athanasiadis, P. J., Gualdi, S., Cassou, C., Castruccio, F., Danabasoglu, G., Davini, P., Dunstone, N., Eade, R., Gastineau, G., Harvey, B., Hermanson, L., Qasmi, S., Ruprich-Robert, Y., Sanchez-Gomez, E., Smith, D., Wild, S., & Zampieri, M. (2021). Atlantic Multidecadal Variability and North Atlantic Jet: A Multimodel View from the Decadal Climate Prediction Project, *Journal of Climate*, 34(1), 347-360, doi:[10.1175/JCLI-D-19-0981.1](https://doi.org/10.1175/JCLI-D-19-0981.1)

Ruprich-Robert, Y., E. Moreno-Chamarro, X. Levine, A. Bellucci, C. Cassou, F. Castruccio, P. Davini, R. Eade, G. Gastineau, L. Hermanson, D. Hodson, K. Lohmann, J. Lopez-Parages, P.-A. Monerie, D. Nicolí, S. Qasmi, C. D. Roberts, E. Sanchez-Gomez, G. Danabasoglu, N. Dunstone, M.

Martin-Rey, R. Msadek, J. Robson, D. Smith and E. Tourigny (2021). Impacts of Atlantic Multidecadal Variability on the Tropical Pacific: a multi-model study. *npj Climate and Atmospheric Science*, 4, 33, doi:10.1038/s41612-021-00188-5.

Summary of results

Part 1 - Predictability of the impacts linked to the Atlantic Multidecadal Variability

The main results to report are related to the first part of the project, related to the impacts of the Atlantic Multidecadal Variability (AMV).

Idealized AMV experiments were performed with EC-Earth3P-HR, the high resolution (ORCA025L75-T511L91) HighResMIP version of EC-Earth (Haarsma et al., 2020). Following the DCP-C protocol (Boer et al. 2016), two sets of ensemble simulations have been conducted, in which time-invariant SST anomalies corresponding to the warm (AMV+) and cold (AMV-) phases of the observed AMV were imposed over the model North Atlantic using SST nudging. To capture the potential response and adjustment of other oceanic basins to the AMV anomalies, the simulations were integrated for 10 years with fixed external forcing conditions. Ensemble simulations of 17 members were performed in order to robustly estimate the climate impacts of the AMV (only 10 of them were performed on CCA). An extensive description of the experimental protocol is provided in the Technical note for AMV DCP-C simulations: <https://www.wcrp-climate.org/wgsip/documents/Tech-Note-1.pdf>. Similar experiments with the standard resolution of EC-Earth3P (ORCA1L75-T255L91) were performed in another supercomputer (Marenostrum 4, BSC) and are used to explore the impacts of model resolution on our ability to capture the observed AMV teleconnections. For those standard resolution experiments we performed 25 ensemble members for both AM+ and AMV-.

Results from the EC-Earth3P and EC-Earth3P-HR experiments show overall very similar results in summer (Figure 1). In particular, in response to a North Atlantic warming of $\sim 0.25^{\circ}\text{C}$ the models simulate a South Atlantic cooling ($\sim -0.05^{\circ}\text{C}$) and a warming in the eastern Indian Ocean and the Maritime Continent ($\sim 0.10^{\circ}\text{C}$; Figure 1ab). Over the Pacific, temperature anomalies project strongly onto the negative phase of the Inter-decadal Pacific Oscillation, with negative SST anomalies in the tropical Pacific that extend toward the pole in both hemispheres in a horseshoe-like pattern that surrounds positive SST anomalies in the west. Over land, models simulate warm anomalies over the Americas reaching up to 0.25°C as well as warming over the Mediterranean region and over the Eurasian continent.

In terms of sea level pressure (Figure 1cd), an AMV warming leads to low pressure anomalies over a large North Atlantic – Europe region, which is mass compensated by high pressure anomalies over the Pacific Ocean, indicating a modification of the Walker Circulation. This is confirmed by the precipitation anomalies (Figure 1ef) that reveal a northward shift of the Inter-Tropical Convergence Zone (ITCZ) over the Atlantic, the eastern Pacific and the Sahel. Negative precipitation anomalies prevail over the western and central tropical Pacific in both hemispheres, which corresponds to a southward tilt of the South Pacific Convergence Zone (SPCZ) and a southward shift of the ITCZ.

Over the extra-tropics, both models simulate a small but significant rainfall increase over the North Atlantic, consistently with the imposed SST warming that increases the evaporation and the amount of precipitable water. The two models also show drier conditions over South and North America in response to a North Atlantic warming, as well as precipitation increase over India, indicating an impact of AMV on the Asian monsoon. We note that the results from our experiments are consistent

with the AMV impacts previously documented in the literature (e.g., Zhang and Delworth 2006; Dong et al. 2006; Zanchettin et al. 2016; Ruprich-Robert et al. 2017, 2018).

During winter, the climate responses to the imposed AMV are comparable between the two models and qualitatively similar to the summertime ones (Figure 2). However, we note a different response in terms of sea level pressure over the extra-tropical North Atlantic sector, with EC-Earth3P simulating negative anomalies centered East of Europe (Figure 2e) and EC-Earth3P-HR simulating positive anomalies centered over the subpolar gyre (Figure 2f). In the multi-model study of Ruggieri et al. (2021), which includes our EC-Earth3P AMV simulations, we investigated the difference of model responses to AMV forcing over this region in winter. We were able to link those different responses to the different model mean states. In particular, we showed that models simulating a more realistic northward excursion of the extra-tropical jet also simulate stronger wind decrease over the North Atlantic subpolar region in response to an AMV warming. This result indicates that mean model biases impact models ability to simulate climate responses to the observed AMV anomalies. Analysis is ongoing to evaluate whether the differences of sea level pressure responses over the North Atlantic between EC-Earth3P and EC-Earth3P-HR are consistent with the results of Ruggieri et al. (2021).

In addition, the amplitude of the central tropical Pacific cooling response to AMV warming is slightly different between our two model resolutions: the NIÑO3.4 SST cooling reaches -0.17°C in EC-Earth3 and -0.12°C in EC-Earth3P-HR. In Ruprich-Robert et al. (2021), we investigated the reasons leading to this different model response comparing 21 AMV simulations performed by 13 different models, including EC-Earth3P and EC-Earth3P-HR. We found that models differ by a factor 10 in simulating the amplitude of the Equatorial Pacific cooling response to observed AMV warming. Using energy constraint approaches, we tracked back the origins of this spread. We found that the large inter-model spread is mainly driven by different amounts of moist static energy injection from the tropical Atlantic surface into the upper troposphere, which is mostly due to different models mean ITCZ positions and strengths. Analytically correcting models for their mean precipitation biases, we reduce this inter-model uncertainty and we quantify that, following an observed 0.26°C AMV warming, the equatorial Pacific cools by 0.11°C with an inter-model standard deviation of 0.03°C .

Overall, the analyses we conducted, including the idealized AMV experiments performed on the ECMWF supercomputer, point to different model representations of the observed AMV climate impacts due to different model mean states. Therefore, the differences seen between EC-Earth3P and EC-Earth3P-HR results cannot be attributed purely to a change of resolution only. To assess in a more robust way the effects of model resolution on the representation of the AMV impacts, we explored the systematic differences between sets of paired AMV experiments performed with the same model but at two different resolutions. For this specific analysis, we compared the results from for different models: CNRM-CM6-1/CNRM-CM6-1-HR, EC-Earth3/EC-Earth3P-HR, ECMWF-IFS/ECMWF-IFS-HR, MetUM-GOML2/MetUM-GOML2-HR and MPI-ESM1-2/MPI-ESM1-2-HR. Using an analysis of variance (ANOVA) to disentangle between the different sources of inter-model spread in the AMV responses, we found in Hodson et al. (2021, submitted to Climate Dynamics) that models responses are generally unchanged by increasing resolution except concerning the northward displacement of the ITCZ in response to an AMV warming, moving further north at higher resolution.

However, we acknowledge that so far we focused on the large-scale impacts of the AMV, for which we found that model mean state variations are likely the most significant source of uncertainty. Resolution may play a greater role for smaller scale processes or extremes, such as hurricanes or temperature extremes. Future studies will examine those impacts. Given the widespread nature of the impacts of the AMV seen in this report, a better understanding of these model uncertainties, combined with good estimates of the future evolution of the AMV are crucial to predict near-term global climate changes.

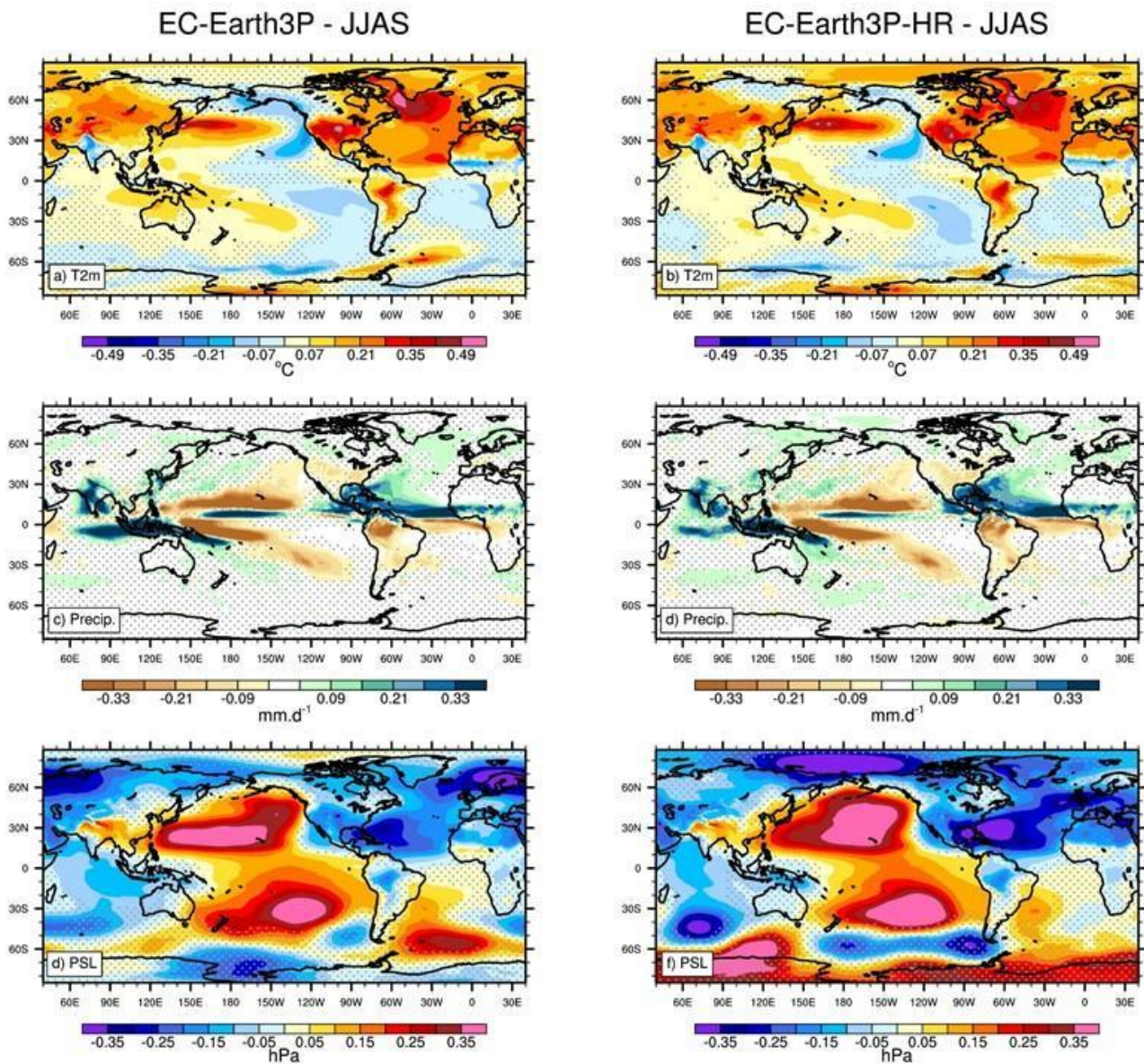


Figure 1: Differences between the 10-yr average of AMV+ and AMV- ensemble simulations for the JJAS season. (a), (b) 2-meter air temperature, (c), (d) precipitation, and ϵ , (f) sea level pressure. Results from (left) EC-Earth3 and (right) EC-Earth3P-HR are shown. Stippling indicates regions that are below the 95% confidence level of statistical significance according to a two-sided Student's t test.

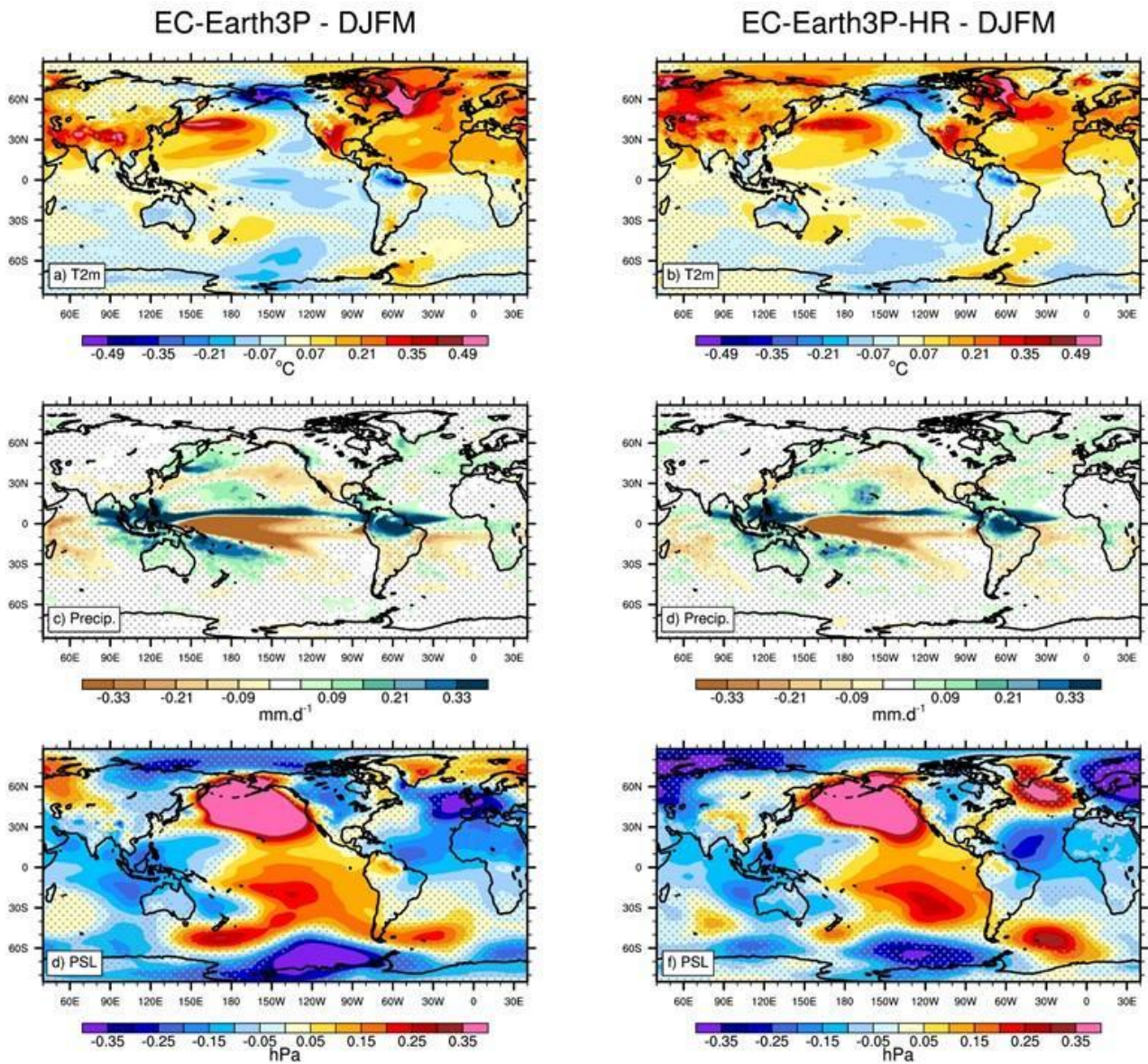


Figure 2: Differences between the 10-yr average of AMV+ and AMV- ensemble simulations for the DJFM season. (a), (b) 2-meter air temperature, (c), (d) precipitation, and (e), (f) sea level pressure. Results from (left) EC-Earth3 and (right) EC-Earth3P-HR are shown. Stippling indicates regions that are below the 95% confidence level of statistical significance according to a two-sided Student's t test.

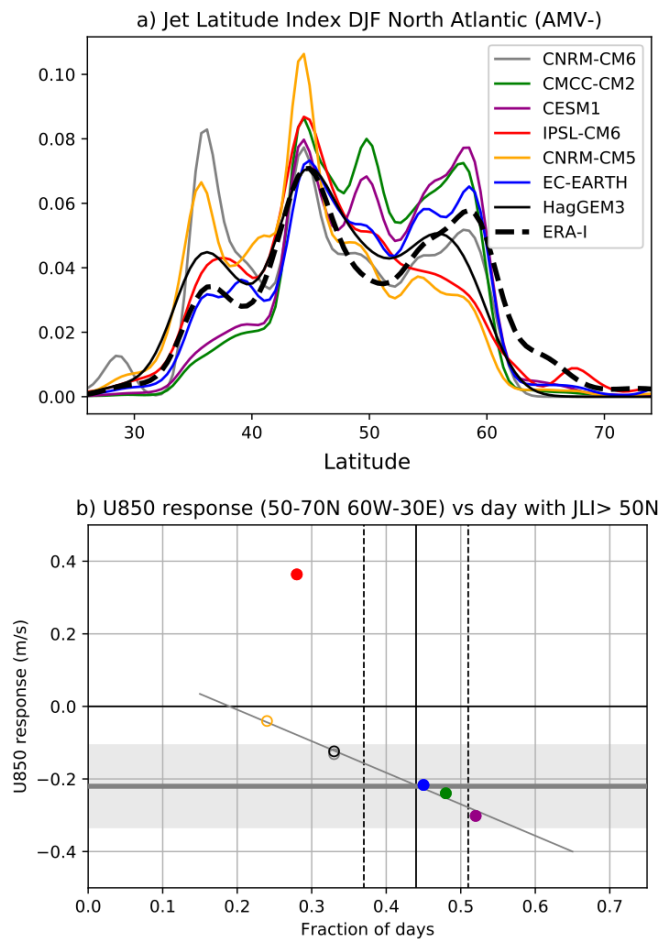


Figure 3: (a) Smooth density of the Jet Latitude Index (JLI) for AMV- experiments (solid lines) and ERA-Interim (bold dashed line) in DJF over the North Atlantic ($30^{\circ}\text{W}-0^{\circ} / 15^{\circ}\text{N}-17^{\circ}\text{N}$). The JLI is defined as the latitude where the jet is maximum over a time running window of 10 days. (b) Relationship between the response of the zonal wind at 850 hPa averaged in the sector $60^{\circ}\text{W}-30^{\circ}\text{E} / 50^{\circ}\text{N}-70^{\circ}\text{N}$ and the fraction of days with $\text{JLI} > 50^{\circ}\text{N}$ in AMV-. A vertical solid line indicates the x value of ERA-Interim. Two dashed vertical lines mark the interval corresponding to one interannual standard deviation in ERA-Interim computed after a 10-yr running mean. Horizontal solid line marks the zero line. A bold, gray horizontal line indicates the value of the multimodel wind response. The shading indicates the confidence interval of the multimodel response. The thin gray line is a linear fit excluding the model with positive response (IPSL-CM6). Models with (without) a statistically significant response of the wind are indicated with a filled (empty) marker. From Ruggieri et al. (2021).

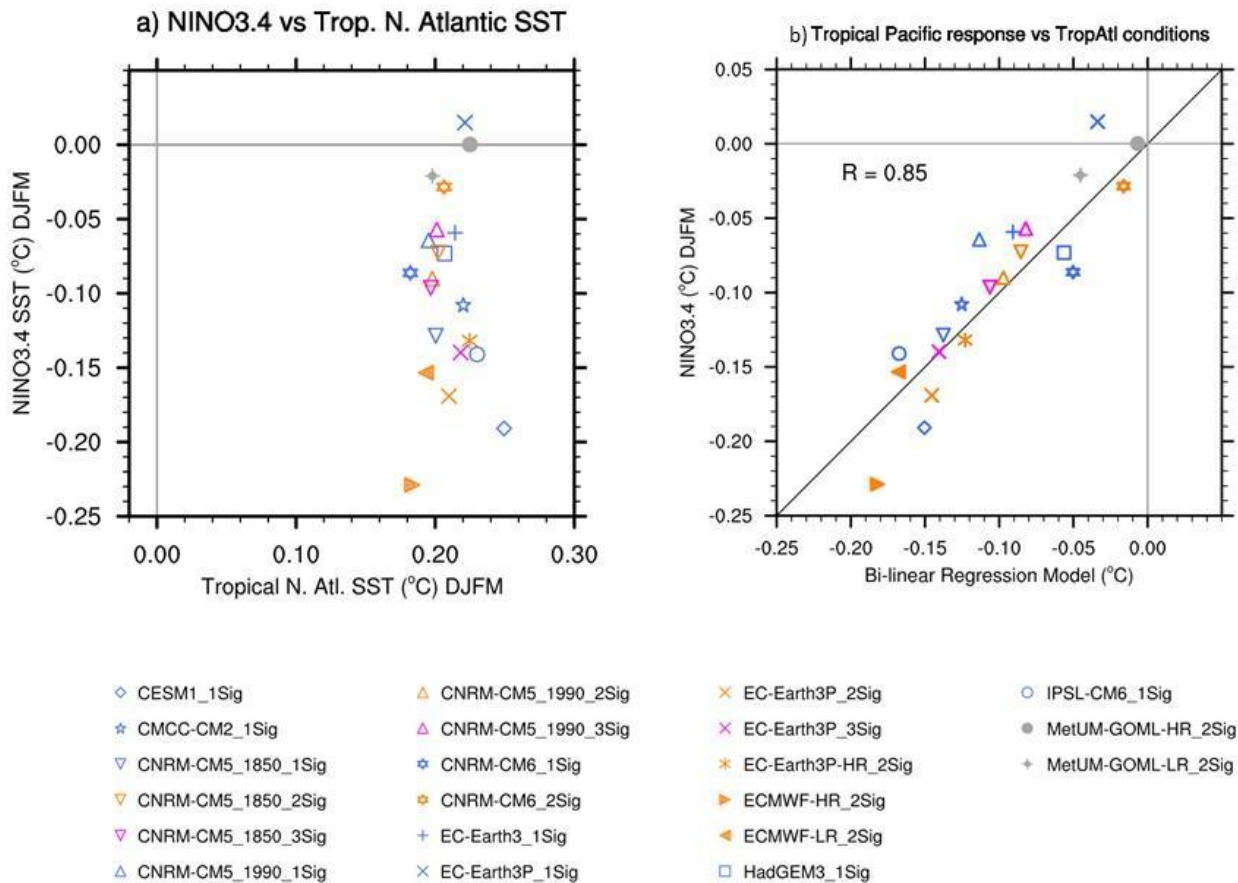


Figure 4: (a) Inter-model relationship between the winter (DJFM) Niño3.4 SST index versus winter tropical North Atlantic SST (averaged over 5°N-20°N / 60°W-10°E). Markers represent the 10-year averaged ensemble mean difference between AM+ and AMV- simulation from individual experiments. (b) Inter-model relationship between the winter (DJFM) Niño3.4 SST index versus a bi-linear regression model using the mean precipitation conditions over the East tropical Pacific and the tropical Atlantic during summer (JJAS) as predictors. From Ruprich-Robert et al. (2021).

Part 2 - Seasonal Forecasts at High Resolution

We now briefly summarise the progress and preliminary steps that were done to be able to execute the HR seasonal predictions envisaged for the second part of the project. These involved a re-tuning exercise, some tests on initialization with the low-resolution version of the model, and some short tests on prediction mode to ensure that the workflow and model setup was working fine. The tests have been done on the ECMWF CCA machine, which accounts for the low SBU usage (2,8M) for the first half of 2021.

The tuning exercise has focused on improving process-representation and mean biases in the Equatorial Pacific and the North Atlantic, two key regions for near-term climate prediction skill. This tuning exercise has been performed over the past year and a half in the BSC supercomputer and has involved the production of more than 15 different experiments and more than 1600 simulation years, which allowed us to define an optimal set of tuning parameters. This process has been slow and time consuming due to, 1) the low production rate (i.e. ~ 3 SYPD) of the high resolution version of EC-Earth, and 2) the need of running several iterations of long sequential in time experiments to optimally adjust the tuning parameters. One particularly interesting feature of this HR model version is the improvement in the simulated variability of the deep convection in the Labrador Sea and the Atlantic Meridional Overturning Circulation (AMOC) compared to the June 2019

standard resolution (SR) version, which occurred too intermittently due to an overly strong local density stratification. The biases in the Labrador Sea caused a problem in the decadal prediction system based on EC-Earth3.3-SR, for which an initialization shock occurred leading to a collapse of the Labrador Sea convection (Bilbao et al, 2021), inducing a quick degradation of the predictive skill in the Subpolar North Atlantic. Some short preliminary tests performed in prediction mode showed that this problem is not present in EC-Earth3.3-HR, for which the Labrador Sea convection remains active and stable, positively impacting the strength of the AMOC (see Figure 5).

Regarding the tests to improve the initialization of the seasonal predictions, these have consisted in a series of reconstructions with the ocean-sea ice standalone LR version of EC-Earth forced with ERA5 surface fluxes, each one following a different assimilation approach. The goal was to find a method to assimilate ORAS5 temperature and salinity information (a reanalysis product of particular interest for having the same resolution as the HR version as EC-Earth), while preventing the inclusion of the non-stationary long-term biases in the western North Atlantic that have been documented for that product (Tietsche et al 2020). The tests included using nudging coefficients of different strength, disabling the nudging at specific regions and/or depths, and combining ORAS5 with other products. The best strategy was selected by performing a series of reduced seasonal prediction systems, each one initialised from one of the tested reconstructions, and computing the associated skill. The best performing approach resulted from combining the assimilation, through nudging of ORAS5 temperature and salinity at the surface and of EN4 temperature and salinity below the mixed layer. As an illustration, Figure 6 shows the skill for predicting ocean temperature and salinity at 500m, for a subset of these test seasonal experiments, in the region where the non-stationary bias in ORAS5 was reported. The strategy that has been finally selected corresponds to the dark green line, which shows persistently high correlation values in the region.

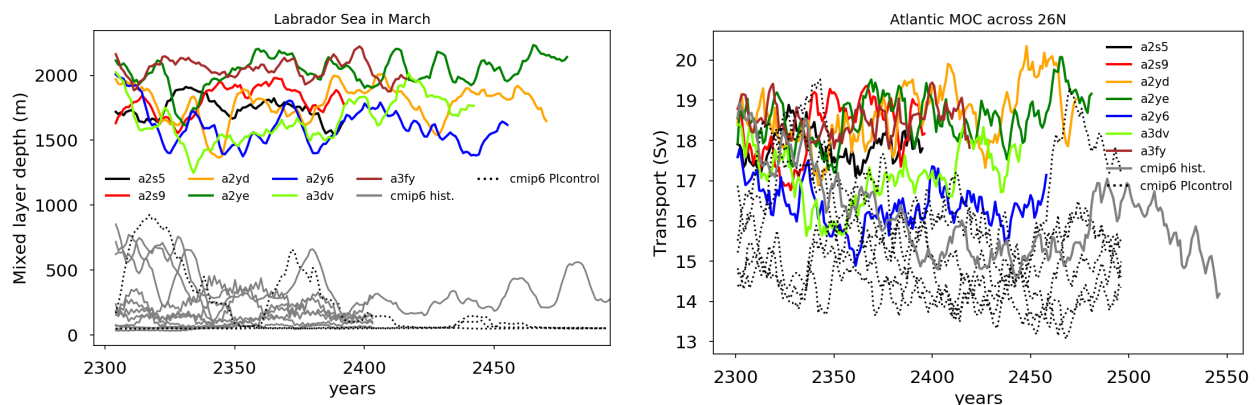


Figure 5: (left) Time-series of the mixed layer depth in the Labrador Sea in March for the different high-resolution experiments with a fixed forcing of the year 1980 (colored lines) compared to the standard-resolution experiments with a fixed forcing of the pre-industrial period (black dashed lines) and with the historical forcing (1850-2014) (grey lines). The mixed layer depth is a proxy of the deep convection of mass waters. (right) Time-series of the AMOC for the same experiments (only one standard resolution experiment with historical forcing - grey line). The decrease in the formation of deep water masses directly impacts the strength of the AMOC. The y-axis on the figures is set arbitrarily.

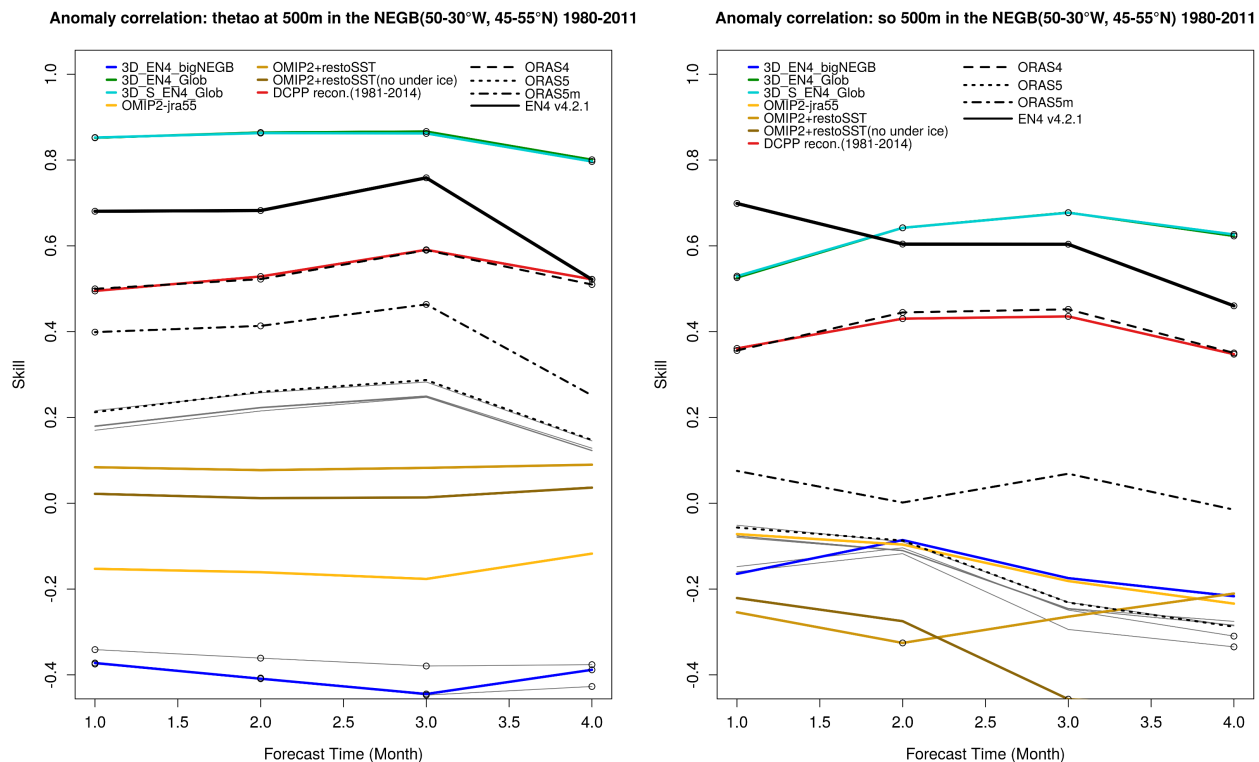


Figure 6: Anomaly correlation coefficient at each forecast month (November through February) of the ocean temperature (left) and salinity (right) in a region North East of the Great Banks in which ORAS5 presents a non-stationary biases, for a selection of seasonal prediction systems initialised following different strategies in the ocean. The skill is evaluated against observations from the Ishii et al. (2005) subsurface temperature and salinity analysis. All predictions are initialised on the 1st of November, have an ensemble size of 5 members and cover the reforecast period 1980-2011.

References

Bilbao, R., S. Wild, P. Ortega, J. Acosta-Navarro, T. Arsouze, P.-A. Bretonnière, L.-P. Caron, M. Castrillo, R. Cruz-García, I. Cvijanovic, F.J. Doblas-Reyes, M. Donat, E. Dutra, P. Echevarría, A.-C. Ho, S. Loosveldt-Tomas, E. Moreno-Chamarro, N. Pérez-Zanon, A. Ramos, Y. Ruprich-Robert, V. Sicardi, E. Tourigny and J. Vegas-Regidor (2021). Assessment of a full-field initialised decadal climate prediction system with the CMIP6 version of EC-Earth. *Earth System Dynamics*, 12, 173-196, doi:10.5194/esd-2020-66.

Boer, G. J., Smith, D. M., Cassou, C., Doblas-Reyes, F., Danabasoglu, G., Kirtman, B., Kushnir, Y., Kimoto, M., Meehl, G. A., Msadek, R., Mueller, W. A., Taylor, K. E., Zwiers, F., Rixen, M., Ruprich-Robert, Y., and Eade, R. (2016) The Decadal Climate Prediction Project (DCPP) contribution to CMIP6, *Geosci. Model Dev.*, 9, 3751–3777, <https://doi.org/10.5194/gmd-9-3751-2016>.

Dong, B., Sutton, R. T., and Scaife, A. A. (2006), Multidecadal modulation of El Niño–Southern Oscillation (ENSO) variance by Atlantic Ocean sea surface temperatures, *Geophys. Res. Lett.*, 33, L08705, doi:[10.1029/2006GL025766](https://doi.org/10.1029/2006GL025766).

Haarsma, R., M. Acosta, R. Bakhshi, P.-A. Bretonnière, L.-P. Caron, M. Castrillo, S. Corti, P. Davini, E. Exarchou, F. Fabiano, U. Fladrich, R. Fuentes Franco, J. García-Serrano, J. von Hardenberg, T. Koenigk, X. Levine, V. Meccia, T. van Noije, G. van den Oord, F.M. Palmeiro, M. Rodrigo, Y. Ruprich-Robert, P. Le Sager, E. Tourigny, S. Wang, M. van Weele and K. Wyser (2020). HighResMIP versions of EC-Earth: EC-Earth3P and EC-Earth3P-HR. Description, model

performance, data handling and validation. *Geoscientific Model Development*, 13, 3507-3527, doi:10.5194/gmd-2019-350.

Ishii, M., M. Kimoto, K. Sakamoto, and S. Iwasaki (2005) Subsurface Temperature And Salinity Analyses. Research Data Archive at the National Center for Atmospheric Research, Computational and Information Systems Laboratory. <https://doi.org/10.5065/Y6CR-KW66>.

Ruprich-Robert, Y., Msadek, R., Castruccio, F., Yeager, S., Delworth, T., & Danabasoglu, G. (2017). Assessing the Climate Impacts of the Observed Atlantic Multidecadal Variability Using the GFDL CM2.1 and NCAR CESM1 Global Coupled Models, *Journal of Climate*, 30(8), 2785-2810, doi:[10.1175/JCLI-D-16-0127.1](https://doi.org/10.1175/JCLI-D-16-0127.1)

Ruprich-Robert, Y., Delworth, T., Msadek, R., Castruccio, F., Yeager, S., & Danabasoglu, G. (2018). Impacts of the Atlantic Multidecadal Variability on North American Summer Climate and Heat Waves, *Journal of Climate*, 31(9), 3679-3700, doi:[10.1175/JCLI-D-17-0270.1](https://doi.org/10.1175/JCLI-D-17-0270.1)

Tietsche, S., M. Balmaseda, H. Zuo, C. Roberts, M. Mayer and L. Ferranti (2020) The importance of North Atlantic Ocean transports for seasonal forecasts. *Clim Dyn* 55, 1995–2011. <https://doi.org/10.1007/s00382-020-05364-6>

Zanchettin, D., Bothe, O., Graf, H. F., Omrani, N.-E., Rubino, A., and Jungclauss, J. H. (2016), A decadal delayed response of the tropical Pacific to Atlantic multidecadal variability, *Geophys. Res. Lett.*, 43, 784–792, doi:[10.1002/2015GL067284](https://doi.org/10.1002/2015GL067284).

Zhang, R., and Delworth, T. L. (2006), Impact of Atlantic multidecadal oscillations on India/Sahel rainfall and Atlantic hurricanes, *Geophys. Res. Lett.*, 33, L17712, doi:10.1029/2006GL026267.